Detection of Hepatic Lesion: Comparison of Free-Breathing and Respiratory-Triggered Diffusion-Weighted MR imaging on 1.5-T MR system

Hye Young Park, Hyeon Je Cho, Eun-mi Kim, Gham Hur, Yong Hoon Kim, Byung Hoon Lee

Purpose : To compare free-breathing and respiratory-triggered diffusion-weighted imaging on 1.5-T MR system in the detection of hepatic lesions.

Materials and Methods : This single-institution study was approved by our institutional review board. Forty-seven patients (mean 57.9 year; M:F = 25:22) underwent hepatic MR imaging on 1.5-T MR system using both free-breathing and respiratory-triggered diffusion-weighted imaging (DWI) at a single examination. Two radiologists retrospectively reviewed respiratory-triggered and free-breathing sets (B50, B400, B800 diffusion weighted images and ADC map) in random order with a time interval of 2 weeks. Liver SNR and lesion-to-liver CNR of DWI were calculated measuring ROI.

Results : Total of 62 lesions (53 benign, 9 malignant) that included 32 cysts, 13 hemangiomas, 7 hepatocellular carcinomas (HCCs), 5 eosinophilic infiltration, 2 metastases, 1 eosinophilic abscess, focal nodular hyperplasia, and pseudolipoma of Glisson's capsule were reviewed by two reviewers. Though not reaching statistical significance, the overall lesion sensitivities were increased in respiratory-triggered DWI [reviewer1: reviewer2, 47/62(75.81%):45/62(72.58%)] than free-breathing DWI [44/62(70.97%):41/62(66.13%)]. Especially for smaller than 1 cm hepatic lesions, sensitivity of respiratory-triggered DWI [24/30(80%):21/30(70%)] was superior to free-breathing DWI [17/30(56.7%):15/30(50%)]. The diagnostic accuracy measuring the area under the ROC curve (Az value) of free-breathing and respiratory-triggered DWI was not statistically different. Liver SNR and lesion-to-liver CNR of respiratory-triggered DWI (87.6±41.4, 41.2±62.5) were higher than free-breathing DWI (38.8±13.6, 24.8±36.8) (p value <0.001, respectively).

Conclusion : Respiratory-triggered diffusion-weighted MR imaging seemed to be better than free-breathing diffusion-weighted MR imaging on 1.5-T MR system for the detection of smaller than 1 cm lesions by providing high SNR and CNR.

Index words : Diffusion-weighted imaging
Magnetic resonance imaging (MRI)
Liver
Single shot EPI

JKSMRM 15:22-31(2011)

Department of Radiology, Ilsan Paik Hospital, Inje University College of Medicine
Received; March 16, 2010, revised; January 13, 2011, accepted; January 17, 2011
Corresponding author : Hyeon Je Cho, M.D., Department of Radiology, Inje University Ilsan-Paik Hospital,
2240 Daehwa-dong, Ilsanseo-gu, Goyang-si, Gyeonggi-do 411-706, Korea.
Tel. 82-31-910-7628 Fax. 82-31-910-7369 E-mail: meditererian@hanmail.net

Introduction

Detection and exact characterization of focal hepatic lesions are important as it would influence not only the treatment decision, but also predicting its prognosis. In the past, CT was regarded as the best choice for the detection of hepatic lesion. Currently Magnetic Resonance Imaging (MRI) is considered more sensitive and specific methods (1, 2). Among the abundant sequences of MR imaging, diffusion-weighted imaging gets spotlights for high contrast resolution as well as its ability to presume the histopathologic architecture or discern the fluid character. Diffusion-weighted imaging (DWI) in the abdomen has had remarkable improvement since the earliest reports (3). However, it is still hard to obtain high-quality image in abdomen by the image distortions due to susceptibility artifacts, chemical shift artifacts induced by abundant peritoneal fat, respiratory motion artifacts and pulsatile flow artifacts from the aorta. In spite of those demerits, there were articles that free-breathing DWI was useful tool for detection and characterization of hepatic lesions such as abscess, metastasis, hemangioma, HCC and cyst (4–6). Recent journals also showed that respiratory-triggered DWI has improved signal-to-noise ratio (SNR) and contrast-to-noise ratio (CNR) of the liver and provided better image quality (7–12). So the application of respiratory-triggered DWI may further improve image quality, spatial resolution and SNR in addition they may enhance the ability to detect and characterize the smaller hepatic lesion (12, 13). In previous study, respiratory-triggered DWI was compared with free-breathing or breath-hold DWI in some specific diseases such as HCC or metastasis (14–17). However, there was a no published study comparing each sequence on the efficiency of the detection of hepatic lesion.

Hence, the aim of this study is to compare respiratory-triggered DWI with free-breathing DWI in terms of the detection of hepatic lesions by using quantitative and qualitative analysis.

Materials and Methods

Subject Population

This single-institution study was approved by our institutional review board. 73 patients had undergone liver MRI on the query of medical database between May 2009 and June 2009. Among them, 26 patients who had not undergone free-breathing DWI or respiratory-triggered DWI were excluded. So we recruited consecutive 47 patients (25 male, 22 female; mean age, 57.9 years; age range, 24–86 years) who had undergone free-breathing DWI and respiratory-triggered DWI of the liver at a single examination. They underwent MRI to characterize liver lesions initially detected on sonography or CT. Some lesions such as small cysts were incidentally found on MRI during the evaluation of the liver or biliary system. It resulted in a total of 62 lesions (53 benign, 9 malignant) that included 32 cysts, 13 hemangiomas, 7 hepatocellular carcinomas (HCCs), 6 focal eosinophilic liver disease, 2 metastases, 1 focal nodular hyperplasia, and pseudolipoma of Glisson's capsule.

The diagnosis was confirmed by all available data in the form of image characteristics, pathology and clinical courses: typical imaging characteristics and clinical courses in all cases of hemangiomas, simple hepatic cysts, focal nodular hyperplasia, eosinophilic abscess and pseudolipoma of Glisson's capsule; and high eosinophil count in eosinophilic infiltration which disappeared on follow-up imaging studies. Among 7 HCCs in 6 patients that had typical imaging features on CT and MRI with high leveled α-fetoprotein, a HCC was proved to be well-differentiated HCC on biopsy and 4 HCCs showed typical radiologic features with size growth-up on serial CTs and MRIs and underwent radiofrequency ablation. 2 HCCs showed dense lipiodol uptakes on follow-up CTs after transarterial chemoembolization that also showed hypervascular staining. 2 metastatic lesions in a patient demonstrated uptakes at follow-up PET/CT with primary tumor (colon cancer). The size of malignant lesion is ranged between 1.0 cm and 1.3 cm. In addition to routine MRI sequences, free-breathing DWI and respiratory-triggered DWI were performed in all patients.

MR Imaging

MR imaging was performed on a 1.5-T system (Magnetom Avanto, Siemens Medical Solutions) with two six-channel body phased array coils anterior and two spine clusters (three channels each) posterior. Three-scan trace diffusion-weighted images were acquired using a single-shot spin-echo echo planar

imaging with GRAPPA. The gradient factors (b values) were 50, 400 and 800 s/mm^2. The technical parameters were as follows: echo time, 75.5 ms; receiver bandwidth, 1630 Hz/pixel; spectral fat saturation; field of view, 30–50 cm; matrix, 192 × 144; number of signal averages, constant 40; threshold noise level, 4; section thickness, 5 mm; intersection gap, 0.5 mm; 32 ±3 sections acquired. The respiratory-triggered single-shot spin echo echoplanar imaging sequence used TR/TE, automatically adapted from each patient's respiration pattern 8422±917 (7310–11082)/75 and free-breathing DWI used TR/TE, 5200/75. For respiratory triggering, prospective acquisition correction (PACE) was implemented. Prior to scanning, patients were asked to perform deep and regular breathing which was checked by the operator on the monitoring screen, and the technicians practiced the patients several times near the table.

These data were acquired during the end-expiratory phase after contrast injection. The respiratory cycle graphs were always stored. Scan times of free-breathing and respiratory-triggered DWI were 180 to 200 seconds and 260 to 320 seconds. ADC map was created of axial images with constant 40 threshold noise levels, using the b-values of 50, 400 and 800 s/mm^2, built in the console.

Image Analysis

Overall data was analyzed both quantitatively and qualitatively. Respiratory-triggered and free-breathing

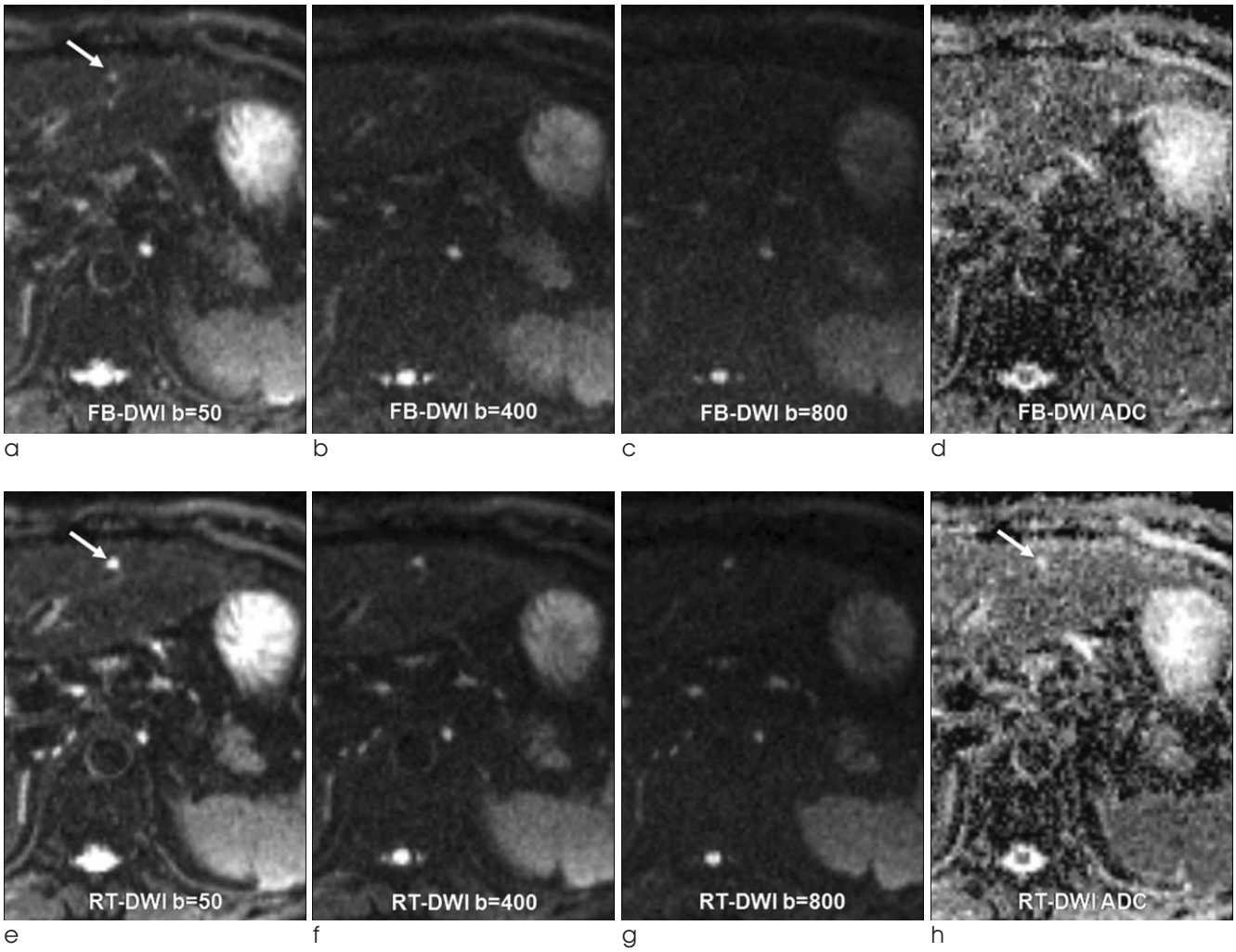

Fig. 1. 64-year-old man with a tiny cyst.
A 0.5 cm cyst (long arrow) was incidentally found during survey of hepatocellular carcinoma (not shown here). It was detected by two reviewers on respiratory-triggered DWI (e to h), but obscure on free-breathing DWI (a to d) and not detected. Note that the lesion was more depictive and brighter on respiratory-triggered DWI.

sets (B50, B400, B800 diffusion images and ADC map) were converted to DICOM files and stored. All informative data were deleted during saving. They were distributed to two reviewers in a random order. Two readers recalled the files on a commercial PACS workstation (5.1 versions, Marotech) and reviewed. The same process was repeated with time interval of 2 weeks. These enabled the reviewers to measure the size and operator-defined regions of interest (ROIs) of the lesion on PACS workstation. Both reviewers were blinded to MR imaging reports, results of other imaging tools, clinical history, laboratory findings and pathologic results. The size and location of lesions (image number and hepatic segment) were recorded by two readers in each case on the free-breathing and respiratory-triggered DWI and ADC map.

Reviewers recorded the presence of each visible abnormality with a five-point confidence scale (1, definitely or almost definitely absent; 2, probably absent; 3, possibly present; 4, probably present, and 5, definitely or almost definitely present). And then, it was analyzed as undetected lesion (1, 2 and 3) and detected lesion (4 and 5) by another radiologist. Qualitative analysis was performed by presence score of depiction of the liver edge and intrahepatic vessels, susceptibility and motion related artifact, and overall image quality on free-breathing and respiratory-triggered DWI by using a four-point confidence scale (1, poor; 2, fair; 3, good; and 4, excellent image quality). All focal hepatic lesions detected by the two reviewers were cross-correlated by an independent radiologist, who reviewed all MRI sequences, other imaging modalities and available clinical variables in order to identify the detected hepatic lesions by two reviewers.

A radiologist performed quantitative comparison of the free-breathing and respiratory-triggered ADC map by analyzing the liver signal-to-noise ratio (SNR) and lesion-to-liver contrast-to-noise ratio (CNR). The liver SNR and lesion-to-liver CNR were calculated using operator-defined ROI measurement of the signal intensity (SI) once each for the liver (SI_{liver}), the lesion (SI_{lesion}) and the background noise (SI_{noise}) in each ADC map. Each operator-defined ROI over 200 mm^2 was placed in the homogeneous liver parenchyma in S5, which was devoid of a large intrahepatic vessel, biliary structure or prominent artifacts. Another operator-defined ROI was placed outside the patient within the line of the phase encoding gradient to measure the system noise at the same image plane. In order to ensure identical placement of the ROI in ADC map, these two sets of images were simultaneously displayed on the workstation and both sets were selected using the ctrl function. Subsequently, ROIs on one image were copied and pasted onto other images of free-breathing and respiratory-triggered sequences at the same site. The site and size of the ROI were therefore identical in each of the free-breathing and respiratory-triggered ADC map. For lesions, a ROI encompassing as much of the lesion as possible was drawn on images, avoiding necrotic or cystic portions of the lesion. The image showing the maximum diameter of the lesion was chosen for drawing the ROI. Cysts and lesions smaller than 0.3 cm were not measured to reassure ROI measurement and standard deviation. 45 lesions were included in analysis finally.

The liver SNR was calculated with the following equation:

$$SNR = SI_{liver} / SI_{noise}$$

The lesion-to-liver CNR was calculated with the following equation:

$$CNR = (SI_{lesion} - SI_{liver}) / SI_{noise}$$

Statistical Analysis

Statistical analysis was performed with MedCalc software (version 9.5, MedCalc, Mariakerke, Belgium). The sensitivity and specificity of each reviewer with free-breathing and respiratory-triggered DWI were calculated separately. The McNemar test was used to analyze the statistical significance of any difference in performance between free-breathing and respiratory-triggered DWI for an individual reviewer. The Independent samples t-test was used to calculate the significance of differences in the values of liver SNR and lesion-to-liver CNR between free-breathing DWI and respiratory-triggered DWI. Receiver operating characteristic (ROC) curve analysis was used to compare the diagnostic capability between respiratory-triggered DWI and free-breathing DWI. The area under the ROC curve (Az value) was used to evaluate the overall diagnostic performance of free-breathing and respiratory-triggered DWI. Wilcoxon rank sum test was used to analyze the statistical significance of qualitative image quality. A p value of < 0.05 was considered significant. To assess interobserver variability in image

interpretation, the κ statistic was used to measure the degree of agreement among multiple observers: A κ value of less than 0.20 indicated poor agreement; a κ value of 0.21–0.40, fair agreement; a κ value of 0.41–0.60, moderate agreement; a κ value of 0.61–0.80, good agreement; and a κ value of more than 0.81,

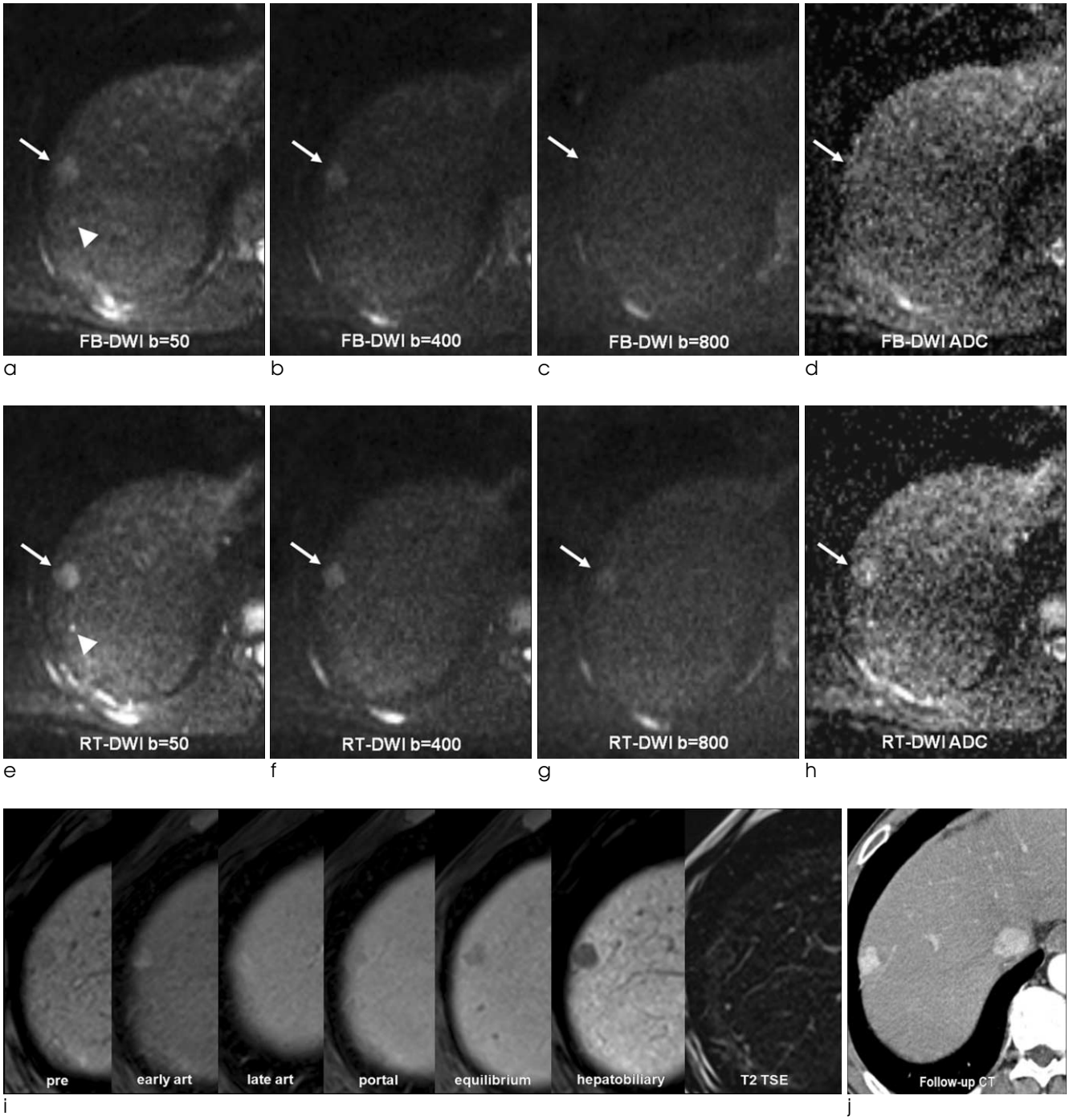

Fig. 2. 52-year-old man with hepatocellular carcinoma.
Both reviewers detected a 1.4 cm hepatocellular carcinoma (long arrow) on free-breathing DWI (a to d) and respiratory-triggered DWI (e to h). However the lesion demonstrated sharper margin and increased CNR on respiratory-triggered DWI. Note the high signals on high b value, representing water restriction. Enhanced dynamic study showed arterial enhancement and early washout (i). HCC had grown on short-term follow-up CT (j) and treated successfully with radiofrequency ablation. Note a tiny cyst (arrowhead) behind HCC.

excellent agreement.

Results

Overall, sensitivity of respiratory-triggered DWI (75.81% and 72.58%) was higher than that of free-breathing DWI (70.97% and 66.13%) for both reviewers. Especially for smaller than 1 cm hepatic lesions, sensitivity of respiratory-triggered DWI (80% and 70%) was much higher than that of free-breathing DWI (56.67% and 50%) (Fig. 1). The sensitivities of each image set for the detection of lesions were summarized in Table 1. Three lesions of pseudolipoma of Glisson's capsule, lipomatous HCC and a metastasis were not detected by two reviewers on free-breathing and respiratory-triggered DWIs. As pseudolipoma of Glisson's capsule was composed of fat that had no T2 and perfusion effects, it was not noted. Lipomatous HCC also had little contrast with the surrounding liver parenchyma. A metastasis was located in S5 subcapsular area beside GB and two reviewers regarded it as bowel or GB fluid in spite of high contrast. 13 cysts less than 1.0 cm in diameter (0.2–0.8 cm) were more detected on respiratory-triggered DWI

Table 1. Sensitivity for the Detection of Hepatic Lesions (n=62)

Size	<1 cm		≥1 cm		Total		p value
Image Set	Free-breathing DWI	Respiratory-triggered DWI	Free-breathing DWI	Respiratory-triggered DWI	Free-breathing DWI	Respiratory-triggered DWI	
Reviwer 1	56.67 (17/30)	80.00 (24/30)	84.38 (27/32)	71.88 (23/32)	70.97 (41/61)	75.81 (47/62)	0.1153
Reviwer 2	50.00 (15/30)	70.00 (21/30)	81.25 (26/32)	75.00 (24/32)	66.13 (41/62)	72.58 (45/62)	0.8036

Note.— *Numbers are the number of true positive lesions.

Table 2. Comparison of Liver SNR and Lesion-to-liver CNR between Free-Breathing and Respiratory-Triggered ADC Map

	Free-breathing ADC map	Respiratory-triggered ADC map	p value
Liver SNR	38.8±46.2	87.6±141.1	<0.001
Lesion-to-liver CNR	24.8±36.8	41.2±62.5	0.001

Note.— Unless otherwise indicated, data are mean ± standard deviations.

Table 3. Az Values Obtained with Free-Breathing and Respiratory-Triggered DWI for the Diagnosis of Hepatic Lesions

	Free-breathing DWI	Respiratory-triggered DWI	p value
Reviewer 1	0.813±0.034	0.752±0.04	0.182
Reviewer 2	0.839±0.032	0.827±0.033	0.746

Note.— Unless otherwise indicated, data are mean ± standard deviations.

Table 4. Comparison of Qualitative Image Study between Free-Breathing and Respiratory-Triggered DWI

	Depiction of the Liver Edge and Intrahepatic Vessels		Motion Related Artifact		Susceptibility Artifact		Overall Image Quality	
Image Set	Free-breathing DWI	Respiratory-triggered DWI	Free-breathing DWI	Respiratory-triggered DWI	Free-breathing DWI	Respiratory-triggered DWI	Free-breathing DWI	Respiratory-triggered DWI
Reviwer 1	3.53±0.65	3.74±0.44	3.74±0.49	3.61±0.74	3.60±0.61	3.70±0.55	3.77±0.48	3.66±0.60
p value	0.05		0.31		0.41		0.33	
Reviwer 2	3.64±0.53	3.70±0.51	3.79±0.41	3.77±0.52	3.72±0.45	3.77±0.43	3.77±0.48	3.74±0.07
p value	0.60		0.84		0.62		0.49	

Note.— Unless otherwise indicated, data are mean image quality scores ± standard deviations.

by two reviewers. Specificity of respiratory-triggered DWI (30.61% and 79.59%) was not significantly different from that of free-breathing DWI (44.9% and 73.47%). Statistical analysis revealed that the mean liver SNR and Lesion-to-liver CNR on respiratory-triggered ADC map was better than that on free-breathing ADC map, although it did not reach the statistical difference (Table 2). Diagnostic accuracies measuring the area under the ROC curve (Az value) were not statistically different (Table 3). Interobserver

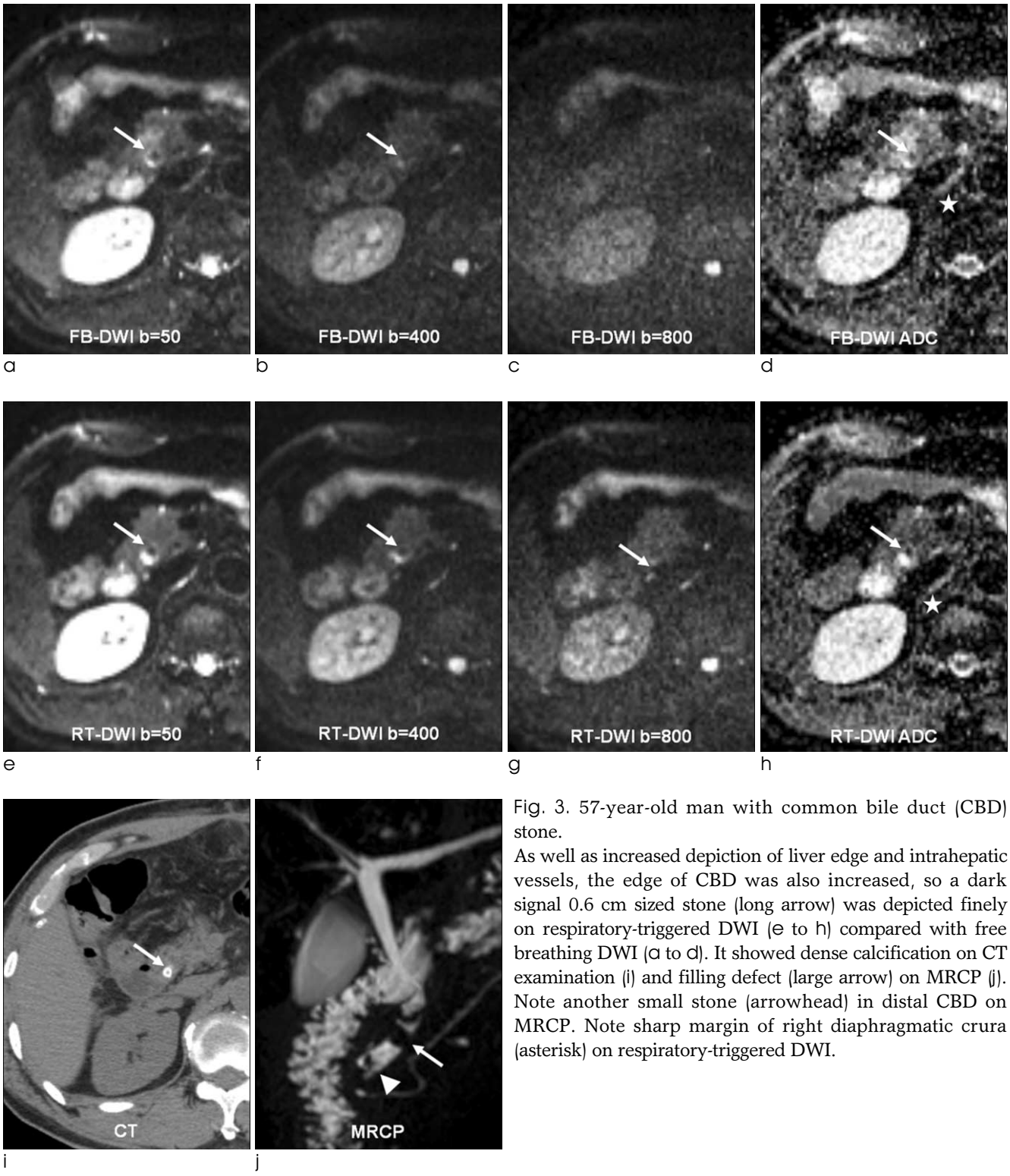

Fig. 3. 57-year-old man with common bile duct (CBD) stone.
As well as increased depiction of liver edge and intrahepatic vessels, the edge of CBD was also increased, so a dark signal 0.6 cm sized stone (long arrow) was depicted finely on respiratory-triggered DWI (e to h) compared with free breathing DWI (a to d). It showed dense calcification on CT examination (i) and filling defect (large arrow) on MRCP (j). Note another small stone (arrowhead) in distal CBD on MRCP. Note sharp margin of right diaphragmatic crura (asterisk) on respiratory-triggered DWI.

agreement for the diagnosis of the hepatic lesions of all sizes was excellent and good agreements for free-breathing (weighted kappa value 0.819) and respiratory-triggered DWI (0.723). Qualitative image study showed better depiction of the liver edge and intrahepatic vessel with statistical significance in a reviewer (Table 4) (Fig. 2).

Discussion

In the detection of hepatic lesions, the overall sensitivity of respiratory-triggered DWI was higher than that of free-breathing DWIfor < 1 cm hepatic lesions. Our results were consistent with already published journals (12, 13, 17). It may be owing to increased lesion-to-liver CNR by improved depiction of the liver edge and intrahepatic vessel. Moreover, the edges of other abdominal organs were also more well demarcated on respiratory-triggered DWI, for example, in biliary system (Fig. 3). However it inevitably demanded a long acquisition time on respiratory-triggered DWI. Additionally, automatically suggested long TR sometimes provided improper image quality with the consequence that acquisition window outlast expiratory phase. Presumably, it resulted in low sensitivity more 1cm lesions on the review. It can be overcome by the use of fixed limited maximum TR which was suggested by other investigators (11).

Our results showed low value of area under the ROC curve (Az value) and specificity of reviewer1 for respiratory-triggered DWI. Considering the higher sensitivity of respiratory-triggered DWI, such low diagnostic performance in terms of Az value and specificity may be owing to increased false-positive of respiratory-triggered DWI. In cases of focal intrahepatic bile duct dilatation by intrahepatic stones or diffuse peripheral intrahepatic duct dilatation associated with Clonorchiasis sinensis infestation, there was markedly increased lesion-to-liver CNR by increased T2 shine through effects. This phenomenon resulted in false positive findings in respiratory-triggered DWI mimicking tiny hepatic cysts or lesions that demand unnecessary efforts to characterize. They were mainly located along portal vein branches and hilar portion. We think that it can be easily overcome with combinational comparison of other T2-weighted images and contiguous survey in stacked image (16, 18).

However, respiratory-triggered DWI has some demerits. The acquisition time of respiratory-triggered DWI is longer than that of free-breathing DWI and our methods are much longer than previous published papers (12, 13). And sometimes respiratory-triggered DWI gave worse image quality than free-breathing DWI. When we met in daily practice, we reviewed the respiratory cycle graph and discussed the cause. The most common cause we encountered, was irregular or shallow breathing patterns in spite of our efforts of explanations and practices before MRI examinations. Coughing, long examination lead time, improper position of respiratory belt checking the movement of abdominal wall and scaphoid abdomen also influenced the image quality (11). The pseudo-anisotropy artifacts were occasionally noted in respiratory-triggered DWI, but it did not affect the interpretation or characterization of lesion (19). As recent liver MRI with liver -specific contrast agents such as gadoxetic acid took long time to get hepatobiliary phase, patents mostly get tired during latter part of the examination. At the beginning part of the study, we acquired DWI after hepatobiliary phase. As we adapted the sequences toward the beginning of the dynamic study, there was improvement. However, this study included all and hence influenced decreased sensitivity and image quality of respiratory-triggered DWI.

Our study has a few potential limitations. Firstly, as in most studies dealing with focal liver lesions, histopathologic confirmation was seldom available. Larger than 2 cm single or two HCCs in a patient underwent radiofrequency ablation without pathologic confirmation according to the guidelines of AASLD and EASL as they did not demand biopsy when CT and MRI findings were concordant with typical imaging features of HCC (20, 21). Obtaining histopathologic diagnosis in all patients would be desirable, but this is not clinically appropriate in most cases. However, a thorough review of all MR sequences and correlation with follow-up imaging and clinical courses may lead to a low probability of misclassification of lesions. Secondly, this study is a retrospective analysis of patients undergoing MR imaging including respiratory-triggered and free-breathing DWI. Thus, there is a possibility of selection bias. Thirdly, this study included too small number of malignant lesions. As the malignant lesion has a tendency to show low or

variable signal than the cyst on ADC map, regardless of DWI, only reflecting the tumor character. Fourthly, we did not compare these DWI sequences with other sequences for the ability to detect and characterize liver lesions because our aim was only to compare two sequences in qualitative and quantitative aspects. Finally, in the era of hepatobiliary agent which is regarded as the most sensitive agent for the detection of hepatic lesions, the usefulness of DWI in that regard might be of concern. However, we should keep in mind that DWI has its own advantages such as non-contrast study and fast acquisition capability, compared to hepatobiliary agent-enhanced MRI.

Conclusion

This study showed that respiratory-triggered DWI was better than free-breathing DWI for hepatic imaging because it provides higher liver SNR and lesion-to-liver CNR and provided better focal hepatic lesion detection, especially for smaller than 1 cm lesion. However, because this study included too small numbers of malignant lesions, further studies using a large scale population should be guaranteed.

References

1. Elsayes KM, Leyendecker JR, Menias CO, et al. MRI characterization of 124 CT-indeterminate focal hepatic lesions: evaluation of clinical utility. HPB (Oxford) 2007;9:208-215
2. Ward J. New MR techniques for the detection of liver metastases. Cancer Imaging 2006;6:33-42
3. Muller MF, Prasad P, Siewert B, Nissenbaum MA, Raptopoulos V, Edelman RR. Abdominal diffusion mapping with use of a whole-body echo-planar system. Radiology 1994;190:475-478
4. Ichikawa T, Haradome H, Hachiya J, Nitatori T, Araki T. Diffusion-weighted MR imaging with a single-shot echoplanar sequence: detection and characterization of focal hepatic lesions. AJR Am J Roentgenol 1998;170:397-402
5. Namimoto T, Yamashita Y, Sumi S, Tang Y, Takahashi M. Focal liver masses: characterization with diffusion-weighted echo-planar MR imaging. Radiology 1997;204:739-744
6. Vossen JA, Buijs M, Liapi E, Eng J, Bluemke DA, Kamel IR. Receiver operating characteristic analysis of diffusion-weighted magnetic resonance imaging in differentiating hepatic hemangioma from other hypervascular liver lesions. J Comput Assist Tomogr 2008;32:750-756
7. Bruegel M, Holzapfel K, Gaa J, et al. Characterization of focal liver lesions by ADC measurements using a respiratory triggered diffusion-weighted single-shot echo-planar MR imaging technique. Eur Radiol 2008;18:477-485
8. Kwee TC, Takahara T, Koh DM, Nievelstein RA, Luijten PR. Comparison and reproducibility of ADC measurements in breathhold, respiratory triggered, and free-breathing diffusion-weighted MR imaging of the liver. J Magn Reson Imaging 2008;28:1141-1148
9. Nasu K, Kuroki Y, Sekiguchi R, Nawano S. The effect of simultaneous use of respiratory triggering in diffusion-weighted imaging of the liver. Magn Reson Med Sci 2006;5:129-136
10. Gourtsoyianni S, Papanikolaou N, Yarmenitis S, Maris T, Karantanas A, Gourtsoyiannis N. Respiratory gated diffusion-weighted imaging of the liver: value of apparent diffusion coefficient measurements in the differentiation between most commonly encountered benign and malignant focal liver lesions. Eur Radiol 2008;18:486-492
11. Kandpal H, Sharma R, Madhusudhan KS, Kapoor KS. Respiratory-triggered versus breath-hold diffusion-weighted MRI of liver lesions: comparison of image quality and apparent diffusion coefficient values. AJR Am J Roentgenol 2009;192:915-922
12. Holzapfel K, Bruegel M, Eiber M, et al. Characterization of small (</=10mm) focal liver lesions: Value of respiratory-triggered echo-planar diffusion-weighted MR imaging. In: Eur J Radiol, 2009
13. Quan XY, Sun XJ, Yu ZJ, Tang M. Evaluation of diffusion weighted imaging of magnetic resonance imaging in small focal hepatic lesions: a quantitative study in 56 cases. Hepatobiliary Pancreat Dis Int 2005;4:406-409
14. Koh DM, Scurr E, Collins DJ, et al. Colorectal hepatic metastases: quantitative measurements using single-shot echo-planar diffusion-weighted MR imaging. Eur Radiol 2006;16:1898-1905
15. Nasu K, Kuroki Y, Nawano S, et al. Hepatic metastases: diffusion-weighted sensitivity-encoding versus SPIO-enhanced MR imaging. Radiology 2006;239:122-130
16. Xu PJ, Yan FH, Wang JH, Lin J, Ji Y. Added value of breathhold diffusion-weighted MRI in detection of small hepatocellular carcinoma lesions compared with dynamic contrast-enhanced MRI alone using receiver operating characteristic curve analysis. J Magn Reson Imaging 2009;29:341-349
17. Bruegel M, Gaa J, Waldt S, et al. Diagnosis of hepatic metastasis: comparison of respiration-triggered diffusion-weighted echo-planar MRI and five t2-weighted turbo spin-echo sequences. AJR Am J Roentgenol 2008;191:1421-1429
18. Parikh T, Drew SJ, Lee VS, et al. Focal liver lesion detection and characterization with diffusion-weighted MR imaging: comparison with standard breath-hold T2-weighted imaging. Radiology 2008;246:812-822
19. Nasu K, Kuroki Y, Fujii H, Minami M. Hepatic pseudo-anisotropy: a specific artifact in hepatic diffusion-weighted images obtained with respiratory triggering. MAGMA 2007;20:205-211
20. Bruix J, Sherman M, Llovet JM, et al. Clinical management of

hepatocellular carcinoma. Conclusions of the Barcelona-2000 EASL conference. European Association for the Study of the Liver. J Hepatol 2001;35:421-430
21. Bruix J, Sherman M. Practice Guidelines Committee, American Association for the Study of Liver Diseases. Management of Hepatocellular carcinoma. Hepatology 2005;42:1208-1236

대한자기공명의과학회지 15:22-31(2011)

국소 간 병변의 발견: 1.5-T 자기공명영상에서의 자유호흡과 호흡유발 확산강조 영상의 비교

인제대학교 일산백병원 영상의학과

박혜영 · 조현제 · 김은미 · 허 감 · 김용훈 · 이병훈

목적: 이 연구의 목적은 간 병변 발견에 있어 1.5-T 자기공명영상에서 자유 호흡 확산강조 영상과 호흡 유발 확산강조 영상의 유용성을 비교하는데 있다.

대상 및 방법: 47명의 환자 (평균 57.9세, 남성:여성 = 25:22)가 한번의 간 자기공명 영상 검사에서 자유호흡 확산강조 영상과 호흡유발 확산 강조 영상을 동시에 시행하였다. 이를 두 명의 영상의학과 의사가 호흡유발 이미지 세트 (B50, B400, B800 확산강조 영상과 ADC map)와 자유호흡 이미지 세트를 2주간의 시간 간격을 두고 무작위로 후향적 분석을 시행하였다. 영상분석을 위하여 특정영역(ROI)를 설정한 후에 간의 신호대 잡음비 (signal-to-noise ratio, SNR)와 대조도(contrast-to-noise ratio, CNR)를 계산하였다.

결과: 32개의 낭종, 13개의 혈관종, 7개의 간세포암, 6 국소 호산구성 간질환, 2개의 전이, 1개의 초점성 결절성 과증식과 글리슨막의 가성지방종을 포함하는 총 62개의 병변이 두 명의 평가자에 의하여 분석되었다. 비록 통계적 유의성을 없었으나, 전체적인 병변 발견의 sensitivity는 호흡유발 확산강조 영상이 〔평가자1:평가자2, 47/62(75.81%):45/62(72.58%)〕 자유호흡 확산강조 영상보다 〔44/62(70.97%):41/62(66.13%)〕 더 높은 수치를 보였다. 특히 1 cm보다 작은 국소 간 병변 발견의 sensitivity는 호흡유발 확산강조 영상이 〔24/30(80%):21/30(70%)〕 자유호흡 확산강조 영상보다 〔17/30(56.7%):15/30(50%)〕 더 우월하였다. 진단적 정확도를 계산하기 위하여 ROC curve (Az value)를 구하였으며 자유호흡 확산강조 영상과 호흡유발 확산강조 영상간에는 통계적 차이는 없었다. 간의 신호대 잡음비 (SNR)와 대조도(CNR)는 호흡유발 확산강조 영상이 (87.6±41.4, 41.2±62.5) 자유호흡 확산강조 영상보다 (38.8±13.6, 24.8±36.8) 높았으며 통계적인 유의성이 있었다. (p value < 0.001).

결론: 1.5-T 자기공명 시스템에서 1 cm보다 작은 간 병변 발견에 있어서 호흡유발 확산강조 영상이 자유호흡 확산강조 영상보다 좋으며 이는 호흡유발 확산강조 영상이 높은 신호대 잡음비 (SNR)와 대조도(CNR)를 보이기 때문이다.

통신저자 : 조현제, (411-706) 경기도 고양시 일산서구 대화동 2240, 인제대학교 일산백병원 영상의학과
Tel. 82-31-910-7628 Fax. 82-31-910-7369 E-mail: mediterenian@hanmail.net